Published in final edited form as:
Cancer Res. 2010 December 15; 70(24): 10351–10361. doi:10.1158/0008-5472.CAN-10-0740.

Combinatorial regulation of neuroblastoma tumor progression by N-Myc and hypoxia inducible factor HIF-1α

Guoliang Qing[1,3], **Nicolas Skuli**[1,3], **Patrick A. Mayes**[2], **Bruce Pawel**[2], **Daniel Martinez**[2], **John M. Maris**[1,2], and **M. Celeste Simon**[1,3,*]

[1]Abramson Family Cancer Research Institute, University of Pennsylvania School of Medicine, Philadelphia, PA 19104, USA

[2]Division of Oncology and Center for Childhood Cancer Research, Children's Hospital of Philadelphia, Department of Pediatrics, University of Pennsylvania School of Medicine, Philadelphia, PA 19104, USA

[3]Howard Hughes Medical Institute, 421 Curie Blvd., Philadelphia, PA 19104, USA

Abstract

In human neuroblastoma, amplification of the *MYCN* gene predicts poor prognosis and resistance to therapy. Because hypoxia contributes to aggressive tumor phenotypes, predominantly via two structurally related hypoxia inducible factors, HIF-1α and HIF-2α, we examined hypoxia responses in *MYCN* amplified neuroblastoma cells. We demonstrate here that HIF-1α, but not HIF-2α, is preferentially expressed in both *MYCN* amplified neuroblastoma cells and primary tumors in comparison to samples without *MYCN* amplification. Our results showed that interplay between N-Myc and HIF-1α plays critical roles in neuroblastoma. For example, high levels of N-Myc override HIF-1α inhibition of cell cycle progression, enabling continued proliferation under hypoxia. Furthermore, both HIF-1α and N-Myc are essential for the Warburg effect (aerobic glycolysis) in neuroblastomas by activating the transcription of multiple glycolytic genes. Of note, expression of Phosphoglycerate Kinase 1 (*PGK1*), Hexokinase 2 (*HK2*) and Lactate Dehydrogenase A (*LDHA*), were each significantly higher in *MYCN* amplified neuroblastomas compared to tumors without *MYCN* amplification. Interestingly, *MYCN* amplified neuroblastoma cells are “addicted” to LDHA enzymatic activity, as its depletion completely inhibits tumorigenesis *in vivo*. Thus, our results provide mechanistic insights explaining how *MYCN* amplified neuroblastoma cells contend with hypoxic stress and paradoxically how hypoxia contributes to neuroblastoma aggressiveness through combinatorial effects of N-Myc and HIF-1α. These results also suggest LDHA represents a novel, pharmacologically tractable target for neuroblastoma therapeutics.

Keywords

N-Myc; hypoxia inducible factor; neuroblastoma; tumorigenesis; Warburg effect

*Corresponding author: M. Celeste Simon, Ph.D., 451 BRB II/III, 421 Curie Blvd., Philadelphia, PA 19104, Phone: 215-746-5532, Fax: 215-746-5511, celeste2@mail.med.upenn.edu.

Disclosure of potential conflicts of interest
The authors declared no potential conflicts of interest.

Introduction

Neuroblastoma is one of the most frequent solid tumors in infants and children (1). Risk factors indicative of poor prognosis include age > 18 months at diagnosis, unfavorable histologic grade, and *MYCN* amplification (1,2). Recent studies demonstrate that mutations in the Anaplastic Lymphoma Kinase (*ALK*) gene cause familial neuroblastoma, while several common polymorphisms, such as those in the BRCA1-associated RING Domain-1 (*BARD1*) gene, influence susceptibility to neuroblastoma (3,4). Nevertheless, *MYCN* amplification remains the most important and reliable oncogenic marker, strongly correlating to advanced stages of disease and poor survival. *MYCN* amplification occurs in 20–25% of patients and is consistently associated with high levels of N-Myc protein (1), which is likely to directly contribute to tumor cell behavior (5). Presumably, N-Myc promotes neuroblastoma tumor progression through regulating and/or cooperating with other oncogenic pathways. However, the exact nature of these pathways remains largely unclear.

Hypoxia, a common feature of solid tumors, contributes to aggressive tumor phenotypes. In an adaptive response to O_2 deprivation, cells alter their gene expression primarily through the activation of hypoxia inducible factor (HIF)-1α and HIF-2α (6). HIFs function as heterodimers in which the O_2-labile α subunits form dimeric complexes with a stable β subunit (also called ARNT) and activate the transcription of genes encoding angiogenic, metabolic, and metastatic factors (6). It is well-known that HIF-1α and HIF-2α share both common and unique target genes (7–9). Although both HIF-α subunits cooperatively regulate genes involved in angiogenesis and metastasis (8), HIF-1α selectively activates genes involved in glycolysis and epigenetics while HIF-2α stimulates *Oct4* and Erythropoietin (*EPO*) expression (7,10–12). Intriguingly, genome-wide analysis of HIF-1α and HIF-2α binding sites across more than 25,500 human gene promoters demonstrated that, despite a large degree of overlap in binding of the two HIF-α isoforms, there are striking differences in gene regulation by HIF-1α and HIF-2α (13), further highlighting the distinct roles of HIF-α in hypoxic adaptation (13,14).

MYC family genes are frequently deregulated in numerous types of human cancer. While *C-MYC* is expressed in a wide variety of human tumors, *MYCN* expression is mostly restricted to tumors derived from the nervous system, such as neuroblastoma (15). Upon forming a binary complex with its partner, Max, Myc activates transcription of target genes involved in cell proliferation, angiogenesis, apoptosis and metabolism (15). “Crosstalk” between the c-Myc and HIF pathways has been clearly documented, but is highly complex and depends on cell type and Myc protein levels (16). In response to hypoxia, cell proliferation decreases through increased expression of p21 and p27 and decreased expression of cyclin D2 and E2F1 as a result of HIF-1α mediated inhibition of c-Myc activity (17,18). In direct contrast to HIF-1α, HIF-2α appears to enhance c-Myc activity in clear cell renal carcinoma cells (ccRCCs) and primary tumors (18,19). However, in Burkitt’s lymphoma cells where c-Myc is over-expressed, HIF-1α actually cooperates with, rather than antagonizes, c-Myc to selectively enhance the expression of Hexokinase 2 (*HK2*), Pyruvate Dehydrogenase Kinase 1 (*PDK1*) and Vascular Endothelial Growth Factor (*VEGF*) (20). It appears that specific target gene promoters, cell types and hypoxic conditions determine the way HIF-1α and HIF-2α engage the c-Myc pathway, resulting in either increased or decreased target gene expression. The complexity of HIF-α/c-Myc interaction raises important questions: do mechanisms involving HIF-α/c-Myc apply to other tumor microenvironments, including neuroblastoma? A previous study suggested that N-Myc and c-Myc only share approximately 40% of their target genes (21); therefore, do HIF-1α and HIF-2α employ similar mechanisms to interact with other Myc family members, such as N-Myc?

HIF-2α has been previously implicated in promoting an aggressive neuroblastoma phenotype (22–24), with HIF-2α (and not HIF-1α) correlating with an unfavorable clinical outcome (24). These studies underscore the importance of discriminating HIF-1α vs. HIF-2α expression *in vivo*. However, the impact of HIF-α on Myc was not addressed and neuroblastomas were not segregated based on *MYCN* amplification status. In an effort to investigate how HIF-α and N-Myc regulate neuroblastoma tumor progression, we systematically analyzed the dynamics of HIF-1α and HIF-2α expression and subsequently evaluated the interaction between HIF-α and N-Myc *in vitro* and *in vivo*. Interestingly, we found that HIF-1α, but not HIF-2α, is preferentially expressed in both *MYCN* amplified neuroblastoma cells and primary tumors in comparison to non-amplified samples. Our data suggest that neuroblastomas can be categorized into two groups based on Myc and HIF-α expression patterns, with N-Myc/HIF-1α cooperating in *MYCN* amplified neuroblastomas while c-Myc/HIF-2α appear to cooperate in *MYCN* single-copy tumors. Our data also suggest small molecules targeting tumor metabolism may be a promising and effective treatment in neuroblastoma patients. Furthermore, this study, combined with a previous report on Burkitt's lymphoma (20), demonstrate that cooperation of *MYC* family genes and HIF-1α may play a global role in human tumor progression.

Materials and Methods

Cell Culture

HCT116 cells were maintained in DMEM medium with 10% FBS, and all the neuroblastoma cells were maintained in RPMI medium containing 10% FBS. For hypoxia treatment, cells were cultured in a hypoxic workstation (Ruskinn Technologies) at 1.5% O_2.

Cell cycle analysis

HCT116 or LAN5 cells were cultured at normoxia or hypoxia for 48 hr before analysis. BrdU incorporation was performed following the standard protocol (Becton Dickinson) after a 30 min pulse with 10 μM BrdU. Cells were stained with Alexa 488 anti-BrdU (Invitrogen) and 0.1 M propidium iodide and analyzed in an LSR FACS machine (Becton Dickinson).

QRT-PCR

Total RNA was extracted from cells with Trizol reagent following the manufacturer's instructions (Invitrogen). cDNA was produced from 1 μg of RNA using Superscript II (Invitrogen) with random hexamer primers (Boehringer Mannheim). Analysis of gene expression was performed in a 7900HT Sequence Detection System by using specific Taqman primers (Applied Biosystems).

shRNA analysis

Specific shRNAs against human HIF-1α, N-Myc and LDHA or a control shRNA were obtained from Open Biosystems. After viral transduction, cells were selected with puromycin (Sigma).

Chromatin immunoprecipitation (ChIP), immunoprecipitation (IP) and Western blot analysis

ChIP was performed following standard protocol from Upstate Biotech. For IP assays, cells were lysed in 25 mM Tris (pH 8.0), 100 mM NaCl, and 1% Triton X-100 containing Complete protease inhibitors (Roche) and 200 μM DFX. For all other Western blots, cells were lysed in RIPA and 50 μg total cellular proteins were used for each blot. Antibodies were used as follows: human HIF-1α (BD, Biosciences), human HIF-2α (Novus NB 100–

122), actin (Sigma AC-15), c-Myc (Santa Cruz N-262 and C-33), and N-Myc (Santa Cruz B8.4.B).

Xenograft tumors

Female BALB/C nude mice (Charles River) were injected s.c. in both flanks with three million Kelly cells (control or LDHA shRNA) diluted in 200 μl PBS containing 50% matrigel (BD Bioscience). Tumor weight was measured at the time of sacrifice.

Immunohistochemistry

Sections of primary neuroblastoma tumors were deparaffinized in xylene and rehydrated in graded alcohols. Endogenous peroxidase activity was blocked by 3% hydrogen peroxide for 20 minutes. Slides were incubated with the antibodies against HIF-1α (Labvision HIF-1A67), and HIF-2α (Novus rabbit polyclonal) overnight at 4 °C. The remaining steps were performed using the DAKO CSA kit. Sections from clear cell renal carcinoma were used as controls for HIF-α staining.

Results

HIF-1α, but not HIF-2α, is preferentially expressed in advanced-stage, *MYCN* amplified neuroblastoma cells

In neuroblastoma cells, HIF-2α was selectively stabilized under physiological O_2 conditions (5% O_2) and governed a prolonged hypoxic adaptation under chronic hypoxia (22). In an effort to evaluate the functional interaction between HIF-α (HIF-1α and HIF-2α) and N-Myc, we first examined HIF-α expression in two *MYCN* amplified cell lines (LAN5 and IMR32) cultured at both 5% O_2 and 1.5% O_2, respectively at different time points. We also examined HIF-α levels in two *MYCN* single-copy cell lines (SHSY5Y and SK-N-SH). Interestingly, unlike *MYCN* single-copy cells, which expressed both HIF-1α and HIF-2α (Figure 1B), the two *MYCN* amplified cell lines selectively expressed HIF-1α (Figure 1A). We expanded our studies of HIF-α expression in a series of *MYCN* amplified and single-copy cell lines at 5% O_2 (Figure S1). HIF-1α was selectively expressed in *MYCN* amplified cells, with the Kelly cell line being the only exception. We then exposed neuroblastoma cell lines to 1.5% O_2 for 24, 48 and 72 hr, respectively. Again, we detected abundant HIF-1α protein in all cell lines tested (Figures 1A, 1B and S2); however, HIF-2α was expressed at very low levels in the majority of *MYCN* amplified cell lines. Moreover, a single-copy line, SK-N-AS, also exhibited undetectable HIF-2α expression under these conditions. Thus, lack of detectable HIF-2α expression in most *MYCN* amplified cells and SK-N-AS cells is largely independent of O_2 concentrations. In contrast to a previous study suggesting that HIF-2α levels remain high while HIF-1α decays (22), we found that chronic hypoxic stress destabilized both HIF-α proteins with similar kinetics in most cell lines (Figures 1A, 1B and S2). In support of our data, several recent studies also independently demonstrated that chronic hypoxia resulted in HIF-1α and HIF-2α degradation with similar kinetics in other contexts (25–27), indicating destabilization of both HIF-α isoforms during chronic hypoxia is a general adaptative mechanism.

The fact that HIF-1α was stabilized while HIF-2α was not in most hypoxic *MYCN* amplified cells suggested HIF-2α expression is specifically silenced at the transcriptional level. To investigate the potential mechanisms involved, we quantitated HIF-1α and HIF-2α mRNA abundance in 13 neuroblastoma cell lines, 9 *MYCN* amplified and 4 single-copy, under normoxia. We chose a single-copy cell line, SHSY5Y, as a control because this line showed abundant HIF-1α and HIF-2α expression under hypoxia. The relative mRNA levels of both HIF-1α and HIF-2α in other neuroblastoma cells were analyzed by QRT-PCR. Consistent with protein expression patterns, there was no dramatic difference between HIF-1α mRNA

abundance in all cell lines tested; however, that of HIF-2α was significantly lower in most *MYCN* amplified cells and the single-copy cell line, SK-N-AS, suggesting that lack of HIF-2α expression is due to low basal mRNA levels (Figure 1C). As all the neuroblastoma cell lines currently available were derived from high-risk tumors, we were unable to compare the relative mRNA levels of HIF-α among different risk groups in cell lines. We therefore analyzed microarray data from 101 primary neuroblastoma tumors ranging from low-risk to high-risk (Figure S3). Interestingly, HIF-1α expression is significantly elevated in the *MYCN* amplified group when compared with *MYCN* single-copy, low-risk tumors (p=0.0201), while that of HIF-2α is lower in *MYCN* amplified tumors (p=0.0611).

Gene function is frequently disrupted by epigenetic alterations. To determine if *HIF2A* was epigenetically silenced, we administered 2 different chemicals affecting chromatin structure, 5-aza-2'-deoxycytidine (DAC), a methyltransferase inhibitor, and trichostatin A (TSA), a histone deacetylase inhibitor, to LAN5 cells in which HIF-2α expression was largely absent (Figure 1D). Genes encoding Caspase 8 (*CASP8*) and Tyrosine 3-Monooxygenase/ tryptophan 5-Monooxygenase activation protein, zeta polypeptide (*YWHAZ*) were used as controls, as *CASP8* is transcriptionally silenced in most *MYCN* amplified cells through a mechanism involving DNA methylation and histone deacetylation (28), while *YWHAZ* is a constitutively expressed "house-keeping" gene. Interestingly, administration of either DAC or TSA significantly increased expression of both *HIF2A* and *CASP8*, and a combination of both chemicals lead to further increases in mRNA levels (Figure 1D). Of note, *YWHAZ* expression was largely unchanged with these treatments, arguing against the notion that increased *HIF2A* expression was due to global activation of transcription. Instead, these data demonstrated that in most *MYCN* amplified cells, synergy of DNA methylation and histone deacetylation silenced *HIF2A* transcription.

HIF-1α, but not HIF-2α, is preferentially expressed in primary *MYCN* amplified neuroblastoma tumors

To confirm that our observations were representative of HIF-α status naturally present in human neuroblastomas, we analyzed HIF-α expression by immunochemistry of primary neuroblastoma tumors. We first evaluated the specificity and efficacy of the antibodies in clear cell renal carcinomas (ccRCCs). *VHL* mutation in ccRCCs leads to constitutive stabilization of HIF-1α and/or HIF-2α (Figure 2 and reference 14). We then analyzed HIF-α levels in 15 neuroblastoma tumors (13 *MYCN* amplified and 2 single-copy) (Figure 2 and supplementary Table 1). Again, HIF-1α, but not HIF-2α, was preferentially expressed in *MYCN* amplified tumors. While HIF-2α was distributed to both the cytoplasm and nucleus, HIF-1α was predominantly located in the nucleus (Figures 2 and data not shown). Taken together, these data demonstrated that HIF-1α, but not HIF-2α, is the primary HIF-α subunit involved in adaptation to hypoxia by *MYCN* amplified tumors.

Proliferation of *MYCN* amplified neuroblastoma cells *in vitro* is, paradoxically, unaltered under hypoxia

Moderate levels of hypoxia (approximately 1.5% O_2) inhibit proliferation through HIF-1α mediated inhibition of c-Myc activity (17,18). As *MYCN* amplified cells preferentially expressed HIF-1α, we examined how these cells responded to O_2 deprivation. Interestingly, we observed no significant change in proliferation of LAN5 cells when cultured at either 1.5% O_2 (Figure 3A) or 0.5% O_2 (Figure S4D). We further analyzed three additional *MYCN* amplified cell lines, and found cell numbers were not decreased by low O_2 (Figures S4A–C). Importantly, *MYCN* amplified neuroblastoma cells are highly dependent on N-Myc activity, as depletion of N-Myc expression significantly decreased their proliferation under either normoxia or hypoxia (Figure 3A). We then assessed cell cycle progression of LAN5 cells by BrdU incorporation. No obvious changes in either G1 or S phase were observed in

LAN5 cells (Figures 3B and 3C), in agreement with cell proliferation as measured by serial cell counting (Figure 3A). Moreover, overexpression of c-Myc rescued proliferation of N-Myc depleted LAN5 cells (Figure 3D), confirming that *MYCN* amplified neuroblastoma cells depend on Myc activity to counteract hypoxic inhibition of cell proliferation.

N-Myc overrides HIF-1α inhibition of cell cycle progression under hypoxia

We hypothesized that high levels of N-Myc counteract HIF-1α inhibition of cell proliferation. Based on this reasoning, we examined the interaction between Myc and its binding partner, Max. We chose HCT116 colon cancer cells for comparison, as it has been previously established that HCT116 cell proliferation is inhibited by hypoxia (17,18). Furthermore, hypoxic HCT116 cells reproducibly exhibit decreased Myc activity and Myc/Max interaction (17,18). Note that HCT116 cells express c-Myc, while LAN5 cells express N-Myc only. We detected specific binding of Myc (c-Myc or N-Myc) to its partner, Max, via immunoprecipitation using antibodies against Max (Figures 4A and B, compare lane 2 with lane 1 in IP panel). In HCT116 cells, chronic hypoxia significantly decreased interaction between c-Myc and Max (Figure 4A, compare lane 4 with lanes 2–3 in IP panel). In contrast, interaction of N-Myc with Max did not obviously change in LAN5 cells after 24hr of hypoxia (Figure 4B, compare lane 4 with lanes 2–3 in IP panel). We did not observe detectable interaction between HIF-1α and Max (Figures 4A and B), as the Max-specific antibody efficiently coprecipitated Myc (c-Myc or N-Myc) but not HIF-1α in either HCT116 or LAN5 cells. Failure to detect Max/HIF-1α interaction was not due to a lack of HIF-1α proteins in the cell lysates (Figures 4A and B, input panels). Moreover, reciprocal immunoprecipitation using HIF-1α specific antibody also failed to pull down Max; instead, abundant HIF-1β (the binding partner of HIF-1α) was coprecipitated (data not shown). We have also been unable to observe detectable interaction between c-Myc and HIF-1α using either endogenous or *in vitro* translated proteins (data not shown). These data indicated that direct disruption of Myc/Max interaction by HIF-1α was unlikely to occur in neuroblastoma cells, as shown for ccRRC (18). Instead, chronic hypoxia decreased c-Myc protein abundance (Figure 4A, compare lanes 2, 3 and 4 in input panel), while that of N-Myc was not obviously changed (Figure 4B, compare lanes 2, 3 and 4 in input panel). Of note, changes in Myc abundance correlated with those of Myc/Max interaction, suggesting that the Myc protein levels *per se* determined the stoichiometry of Myc/Max complexes in hypoxic colon carcinoma and neuroblastoma cells.

To confirm whether these *in vitro* results reflected the situation *in vivo*, we assessed Myc occupancy of target gene promoters by ChIP assays, and the relative binding was quantified by QRT-PCR. Consistently, binding of c-Myc to target gene promoters in HCT116 cells did not appreciably change at 6 hr of hypoxia (data not shown), but significantly decreased at 24 hr (Figure 4C). In contrast, hypoxia failed to decrease the binding of N-Myc to target gene promoters at either time point (Figure 4C and data not shown). We next tested hypoxic regulation of Myc targets involved in cell cycle progression: p21 and p27 (repressed by Myc), as well as E2F1 and cyclin D2 (activated by Myc). Under the conditions described above, we observed increased p21 and p27 mRNA expression and decreased cyclin D2 and E2F1 mRNA level in hypoxic HCT116 cells at 24 hr (Figure 4D). When the same target genes were tested, hypoxic LAN5 cells exhibited no detectable changes in their mRNA abundance (Figure 4D). As a positive control, hypoxia significantly increased VEGF expression in either cell line (Figure 4D). Taken together, these results provided novel mechanistic insights explaining how *MYCN* amplified neuroblastoma cells thrive under hypoxic stress.

Both N-Myc and HIF-1α regulate the Warburg effect of Neuroblastoma

Neuroblastomas, like all solid tumors, must meet specific metabolic requirements to fuel their deregulated growth and invasion into surrounding tissues. When O_2 is abundant, differentiated cells extract energy primarily from glucose by oxidative phosphorylation, whereas most (60–70%) tumor cells consume glucose more avidly, converting it to lactate (29,30). This long-observed phenomenon is known as aerobic glycolysis (the Warburg effect). To investigate whether *MYCN* amplified neuroblastoma cells exhibit the Warburg phenotype, we measured glucose uptake and consequent lactate production in 5 cell lines at 21% O_2 (Figure 5A). All cell lines predominantly exhibited a glycolytic metabolism, as they released an average of 1.6 molecules lactate for each glucose molecule consumed.

We then sought to investigate the mechanisms whereby neuroblastoma cells promoted aerobic glycolysis. In this regard, immunostaining of primary neuroblastoma tumors showed that HIF-1α is robustly expressed in multiple distinct tumor areas (Figure 2). One consequence of HIF-1α activation is the stimulation of glycolysis and angiogenesis through increased transcription of glycolytic and angiogenic genes (6). In *MYCN* amplified neuroblastomas, amplification of the *MYCN* gene frequently results in high N-Myc protein levels. Although c-Myc clearly stimulates glycolysis (31), no detailed study has shown that N-Myc acts similarly in this process, as genome-wide analysis of gene expression associated with N-Myc over-expression in either cell lines or primary tumors demonstrated that N-Myc predominantly regulates genes involved in cell cycle progression and ribosome biogenesis (21,32). Moreover, N-Myc and c-Myc only share approximately 40% of their target genes, none of which included genes involved in glycolysis based on this analysis (21). For this purpose, we depleted the expression of N-Myc and HIF-1α, respectively, by specific shRNAs in LAN5 cells (Figures 5B and S5). Knockdown of N-Myc selectively decreased expression of genes encoding Glucose Transporter 1 (*GLUT1*), *HK2*, *PDK1*, *PGK1*, Aldolase A Fructose-Bisphosphate (*ALDA*) and *LDHA* at normoxia, but had no obvious effect on that of *GAPDH* (Figure 5B). Interestingly, HIF-1α depletion (Figure S5) specifically decreased the expression of *GAPDH*, *HK2*, *PDK1*, *ALDA*, and *LDHA* at normoxia (Figure 5C). Simultaneous knockdown of N-Myc and HIF-1α indicated that they additively regulate *HK2* and *LDHA* expression, as inhibiting both factors resulted in a further decrease in expression (Figure 5D). As shown in Figure 4, HIF-1α and N-Myc do not form a physical interaction. However, *HK2*, *PDK1*, and *LDHA* harbor HREs and E boxes in close proximity to each other (20). Taken together, our data and data from the Dang lab (20) suggest that overexpressed Myc and HIF-1α converge on the promoters of these genes to regulate their transcription, thereby combining in the transactivation of some common targets.

As stated above, *MYCN* amplified neuroblastoma cells preferentially express HIF-1α, not HIF-2α. To determine what impact HIF-2α would have on *MYCN* amplified neuroblastoma cells, we stably transfected a plasmid expressing wild-type HIF-2α into *MYCN* amplified cells to mimic “reactivation” of endogenous HIF-2α (Figure S6A). We first examined the expression of numerous HIF-α target genes at 1.5% O_2 (Figure S6B). Expression of HIF-2α further increased *GLUT1* expression, but had no effect on other glycolytic genes (Figure S6B), demonstrating that HIF-1α, but not HIF-2α, predominantly controls expression of glycolytic genes in neuroblastoma. We then analyzed glucose consumption (Figure S6C). Interestingly, HIF-2α expression did not increase glucose uptake when compared with controls. We did observe that hypoxia significantly increases glucose consumption by both control and HIF-2α transfected cells, suggesting that HIF-1α is sufficient to maintain the glycolytic phenotype of neuroblastoma cells under hypoxia. In addition, HIF-2α had no detectable effect on cell cycle progression under hypoxia (Figure S6D). Consistent with these *in vitro* data, HIF-2α expression had no obvious impact on the tumorigenic capacity of SK-N-BE2 cells in a xenograft tumor model (Figure S6E). Taken together, these data

suggest that the function of HIF-1α and HIF-2α is redundant in *MYCN* amplified neuroblastomas, and that HIF-1α plays the dominant role in these tumors. Even if HIF-2α were "reactivated", it would not necessarily result in a dramatic phenotype because of the high levels of HIF-1α present.

LDHA is a promising therapeutic target for *MYCN* amplified neuroblastomas

Based on the data shown above, we analyzed the expression of glycolytic genes in 101 primary neuroblastoma tumors (33). Interestingly, expression of *LDHA*, *HK2* and *PGK1* was significantly up-regulated in *MYCN* amplified tumors when compared with *MYCN* single copy samples (Figure 6A and data not shown). We were particularly interested in LDHA for the following reasons: (1) LDHA expression is significantly up-regulated in *MYCN* amplified neuroblastoma subclass (Figure 6A); (2) it was shown to maintain the Warburg phenotype in other tumor contexts (34,35); and (3) individuals lacking LDHA expression have no obvious phenotype under normal conditions (36). Based on this reasoning, we depleted LDHA expression in two *MYCN* amplified cell lines, LAN5 and Kelly, by means of specific shRNAs (Figure 6B). Strikingly, both cell lines exhibited addiction to LDHA activity as depletion of its expression significantly inhibited their proliferation at normoxia (Figure 6B). More importantly, depletion of LDHA completely inhibited the tumorigenic capacity of Kelly cells *in vivo* (Figure 6C). Taken together, these data suggest that targeting LDHA may provide an effective, non-toxic approach to neuroblastoma therapy.

Discussion

In this study, we identified a previously underappreciated role for N-Myc/HIF-1α cooperation in neuroblastoma tumor progression. Based on these data, we propose the following model (Figure 6D): under normoxia, N-Myc promotes proliferation of neuroblastoma cells by activating genes involved in cell cycle progression. Meanwhile, both N-Myc and low levels of HIF-1α cooperatively contribute to the Warburg effect via regulation of glycolytic genes. Under hypoxia, HIF-1α is further stabilized due to decreased protein degradation. On one hand, high levels of N-Myc protein resulting from genomic amplification override HIF-1α inhibition of cell cycle progression, enabling sustained cell proliferation. On the other, stabilized HIF-1α, together with N-Myc, further increases glucose uptake with concomitant lactate production. It should be noted that N-Myc and HIF-1α may also cooperatively contribute to other processes, such as angiogenesis.

The Warburg effect has been inferred in many cancers by fluorodeoxyglucose positron emission tomography (FDG-PET) (37). Indeed, increased glycolytic capability and overall tumor aggressiveness is being recognized as a common trait of most solid tumors. We demonstrated here that N-Myc and HIF-1α cooperatively contribute to the Warburg effect of neuroblastoma (Figures 5 and 6). Advanced-stage neuroblastomas with *MYCN* amplification are often resistant to conventional therapeutic drugs because of aberrations in their apoptotic machinery (38), making the search for novel druggable targets in this tumor type critical. Systemic inhibition of c-Myc in a Ras-induced lung adenocarcinoma mouse model indicated the feasibility of targeting c-Myc, a common downstream conduit for many oncogenic signals, as an efficient and tumour-specific cancer therapy (39); however, small molecules targeting non-kinase oncogenes like *MYC* have never been achieved. *MYCN* amplified neuroblastomas are highly vascular (1). In principle, blocking angiogenesis (e.g. using anti-VEGF agents) may provide an alternative promising therapeutic approach. Nevertheless, recent studies demonstrated that anti-angiogenesis agents significantly increased invasion and metastasis in a number of tumor models (40,41), somewhat decreasing the enthusiasm of targeting angiogenesis for treatment of cancers like neuroblastoma. Many cancer cells avidly take up glucose and generate lactate through LDHA. However, whether LDHA plays a more general role in tumor progression is still largely unknown, given that 30–40% human

tumors do not exhibit a Warburg phenotype. In this study, we first systematically analyzed a series of *N-MYC* amplified neuroblastoma cells and showed they consistently exhibit a Warburg phenotype. We then demonstrated that targeting LDHA could be another attractive approach in treating neuroblastoma patients with *MYCN* amplification, given that small molecule inhibitors against LDHA are already available (42). Because *MYCN* single-copy neuroblastomas frequently express c-Myc (but not N-Myc) (43), conceivably, c-Myc and HIF-2α cooperate as shown for ccRCCs (18). Thus, we propose that neuroblastomas can be categorized into two groups based on Myc and HIF-α expression patterns, with N-Myc/HIF-1α cooperating in *MYCN* amplified neuroblastomas while c-Myc/HIF-2α cooperate in *MYCN* single-copy tumors. Inhibitors targeting metabolism, either alone or in combination with other chemotherapeutic drugs, should be considered for translation into clinical trials for neuroblastoma patients.

Supplementary Material

Refer to Web version on PubMed Central for supplementary material.

Acknowledgments

We thank members of the Simon lab for helpful suggestions. This work was supported by the Howard Hughes Medical Institute, NIH Grant CA104838 (to M.C. Simon), NIH grant CA097323 (to J.M. Maris) and NIH F32 Training Grant 1F32CA137988 (to G.L. Qing). M.C. Simon is an Investigator of the Howard Hughes Medical Institute.

References

1. Maris JM, Hogarty MD, Bagatell R, Cohn SL. Neuroblastoma. Lancet. 2007; 369:2106–2120. [PubMed: 17586306]
2. Mahller YY, Williams JP, Baird WH, et al. Neuroblastoma cell lines contain pluripotent tumor initiating cells that are susceptible to a targeted oncolytic virus. Plos One. 2009; 1:1–10.
3. Mossé YP, Laudenslager M, Longo L, et al. Identification of ALK as a major familial neuroblastoma predisposition gene. Nature. 2008; 455:930–935. [PubMed: 18724359]
4. Capasso M, Devoto M, Hou C, et al. Common variations in BARD1 influence susceptibility to high-risk neuroblastoma. Nat Genet. 2009; 41:718–723. [PubMed: 19412175]
5. Weiss WA, Aldape K, Mohapatra G, Feuerstein BG, Bishop JM. Targeted expression of MYCN causes neuroblastoma in transgenic mice. EMBO J. 1997; 16:2985–2995. [PubMed: 9214616]
6. Simon MC, Keith B. The role of oxygen availability in embryonic development and stem cell function. Nat Rev Mol Cell Biol. 2008; 9:285–296. [PubMed: 18285802]
7. Hu CJ, Wang LY, Chodosh LA, Keith B, Simon MC. Differential roles of hypoxia-inducible factor 1alpha (HIF-1alpha) and HIF-2alpha in hypoxic gene regulation. Mol Cell Biol. 2003; 23:9361–9374. [PubMed: 14645546]
8. Qing G, Simon M. Hypoxia inducible factor-2alpha: a critical mediator of aggressive tumor phenotypes. Curr Opin Genet Dev. 2009; 19:60–66. [PubMed: 19167211]
9. Sowter HM, Raval RR, Moore JW, Ratcliffe PJ, Harris AL. Predominant role of hypoxia-inducible transcription factor (Hif)-1alpha versus Hif-2alpha in regulation of the transcriptional response to hypoxia. Cancer Res. 2003; 63:6130–6134. [PubMed: 14559790]
10. Covello KL, Kehler J, Yu H, et al. HIF-2alpha regulates Oct-4: effects of hypoxia on stem cell function, embryonic development, and tumor growth. Genes Dev. 2006; 20:557–570. [PubMed: 16510872]
11. Xia X, Lemieux ME, Li W, et al. Integrative analysis of HIF binding and transactivation reveals its role in maintaining histone methylation homeostasis. Proc Natl Acad Sci U S A. 2009; 106:4260–4265. [PubMed: 19255431]

12. Gruber M, Hu CJ, Johnson RS, Brown EJ, Keith B, Simon MC. Acute postnatal ablation of Hif-2alpha results in anemia. Proc Natl Acad Sci U S A. 2007; 104:2301–2306. [PubMed: 17284606]
13. Mole DR, Blancher C, Copley RR, et al. Genome-wide association of hypoxia-inducible factor (HIF)-1alpha and HIF-2alpha DNA binding with expression profiling of hypoxia-inducible transcripts. J Biol Chem. 2009; 284:16767–16775. [PubMed: 19386601]
14. Wiesener MS, Berger I, Morgan NV, et al. Constitutive activation of hypoxia-inducible genes related to overexpression of hypoxia-inducible factor-1alpha in clear cell renal carcinomas. Cancer Res. 2001; 61:5215–5222. [PubMed: 11431362]
15. Adhikary S, Eliers M. Transcriptional regulation and transformation by Myc proteins. Nat Rev Mol Cell Biol. 2005; 6:635–645. [PubMed: 16064138]
16. Dang CV, Kim JW, Gao P, Yustein J. The interplay between MYC and HIF in cancer. Nat Rev Cancer. 2008; 8:51–56. [PubMed: 18046334]
17. Koshiji M, Kageyama Y, Pete EA, Horikawa I, Barrett JC, Huang LE. HIF-1alpha induces cell cycle arrest by functionally counteracting Myc. EMBO J. 2004; 23:1949–1956. [PubMed: 15071503]
18. Gordan JD, Bertout JA, Hu CJ, Diehl JA, Simon MC. HIF-2alpha promotes hypoxic cell proliferation by enhancing c-myc transcriptional activity. Cancer Cell. 2007; 11:335–347. [PubMed: 17418410]
19. Gordan JD, Lai P, Dondeti VR, et al. HIF-alpha effects on c-Myc distinguish two subtypes of sporadic VHL-deficient clear cell renal carcinoma. Cancer Cell. 2009; 14:435–446. [PubMed: 19061835]
20. Kim JW, Gao P, Liu YC, Semenza GL, Dang CV. Hypoxia-inducible factor 1 and dysregulated c-Myc cooperatively induce vascular endothelial growth factor and metabolic switches hexokinase 2 and pyruvate dehydrogenase kinase 1. Mol Cell Biol. 2007; 27:7381–7393. [PubMed: 17785433]
21. Boon K, Caron HN, van Asperen R, et al. N-myc enhances the expression of a large set of genes functioning in ribosome biogenesis and protein synthesis. EMBO J. 2001; 20:1383–1393. [PubMed: 11250904]
22. Holmquist-Mengelbier L, Fredlund E, Löfstedt T, et al. Recruitment of HIF-1alpha and HIF-2alpha to common target genes is differentially regulated in neuroblastoma: HIF-2alpha promotes an aggressive phenotype. Cancer Cell. 2006; 10:413–423. [PubMed: 17097563]
23. Pietras A, Hansford LM, Johnsson AS, et al. HIF-2alpha maintains an undifferentiated state in neural crest-like human neuroblastoma tumor-initiating cells. Proc Natl Acad Sci U S A. 2009; 106:16805–16810. [PubMed: 19805377]
24. Noguera R, Fredlund E, Piqueras M, et al. HIF-1alpha and HIF-2alpha are differentially regulated in vivo in neuroblastoma: high HIF-1alpha correlates negatively to advanced clinical stage and tumor vascularization. Clin Cancer Res. 2009; 15:7130–7136. [PubMed: 19903792]
25. Ginouvès A, IIC K, Macías N, Pouysségur J, Berra E. PHDs overactivation during chronic hypoxia "desensitizes" HIFalpha and protects cells from necrosis. Proc Natl Acad Sci U S A. 2008; 105:4745–4750. [PubMed: 18347341]
26. Rius J, Guma M, Schachtrup C, et al. NF-kappaB links innate immunity to the hypoxic response through transcriptional regulation of HIF-1alpha. Nature. 2008; 453:807–811. [PubMed: 18432192]
27. Zhao T, Zhang CP, Liu ZH, et al. Hypoxia-driven proliferation of embryonic neural stem/progenitor cells--role of hypoxia-inducible transcription factor-1alpha. FEBS J. 2008; 275:1824–1834. [PubMed: 18341590]
28. Hoebeeck J, Michels E, Pattyn F, et al. Aberrant methylation of candidate tumor suppressor genes in neuroblastoma. Cancer Lett. 2008; 273:336–346. [PubMed: 18819746]
29. Vander Heiden MG, Cantley LC, Thompson CB. Understanding the Warburg effect: the metabolic requirements of cell proliferation. Science. 2009; 324:1029–1033. [PubMed: 19460998]
30. Hsu PP, Sabatini D. Cancer cell metabolism: Warburg and beyond. Cell. 2008; 134:703–707. [PubMed: 18775299]
31. Dang CV, O'Donnell KA, Zeller KI, Nguyen T, Osthus RC, Li F. The c-Myc target gene network. Semin Cancer Biol. 2006; 16:253–264. [PubMed: 16904903]

32. Alaminos M, Mora J, Cheung NK, et al. Genome-wide analysis of gene expression associated with MYCN in human neuroblastoma. Cancer Res. 2003; 63:4538–4546. [PubMed: 12907629]
33. Wang Q, Diskin S, Rappaport E, et al. Integrative genomics identifies distinct molecular classes of neuroblastoma and shows that multiple genes are targeted by regional alterations in DNA copy number. Cancer Res. 2006; 66:6050–6062. [PubMed: 16778177]
34. Fantin VR, St-Pierre, Leder P. Attenuation of LDH-A expression uncovers a link between glycolysis, mitochondrial physiology, and tumor maintenance. Cancer Cell. 2006; 9:425–434. [PubMed: 16766262]
35. Shim H, Dolde C, Lewis BC, et al. c-Myc transactivation of LDH-A: implications for tumor metabolism and growth. Proc Natl Acad Sci U S A. 1997; 94:6658–6663. [PubMed: 9192621]
36. Nishimura Y, Honda N, Ohyama K, et al. Lactate dehydrogenase A subunit deficiency. Isozymes Curr Top Biol Med Res. 1983; 11:51–64. [PubMed: 6642993]
37. Gatenby RA, Gillies RJ. Why do cancers have high aerobic glycolysis? Nat Rev Cancer. 2004; 4:891–899. [PubMed: 15516961]
38. Teitz T, Wei T, Valentine MB, et al. Caspase 8 is deleted or silenced preferentially in childhood neuroblastomas with amplification of MYCN. Nature. 2000; 6:529–535.
39. Soucek L, Whitfield J, Martins CP, et al. Modelling Myc inhibition as a cancer therapy. Nature. 2008; 455:679–683. [PubMed: 18716624]
40. Ebos JM, Lee CR, Cruz-Munoz W, Bjarnason GA, Christensen JG, Kerbel RS. Accelerated metastasis after short-term treatment with a potent inhibitor of tumor angiogenesis. Cancer Cell. 2009; 15:232–239. [PubMed: 19249681]
41. Pàez-Ribes M, Allen E, Hudock J, et al. Antiangiogenic therapy elicits malignant progression of tumors to increased local invasion and distant metastasis. Cancer Cell. 2009; 15:3384–3395.
42. Le A, Cooper CR, Gouw AM, et al. Inhibition of lactate dehydrogenase A induces oxidative stress and inhibits tumor progression. Proc Natl Acad Sci U S A. 2010; 107:2037–2042. [PubMed: 20133848]
43. Liu X, Mazanek P, Dam V, et al. Deregulated Wnt/beta-catenin program in high-risk neuroblastomas without MYCN amplification. Oncogene. 2008; 27:1478–1488. [PubMed: 17724465]

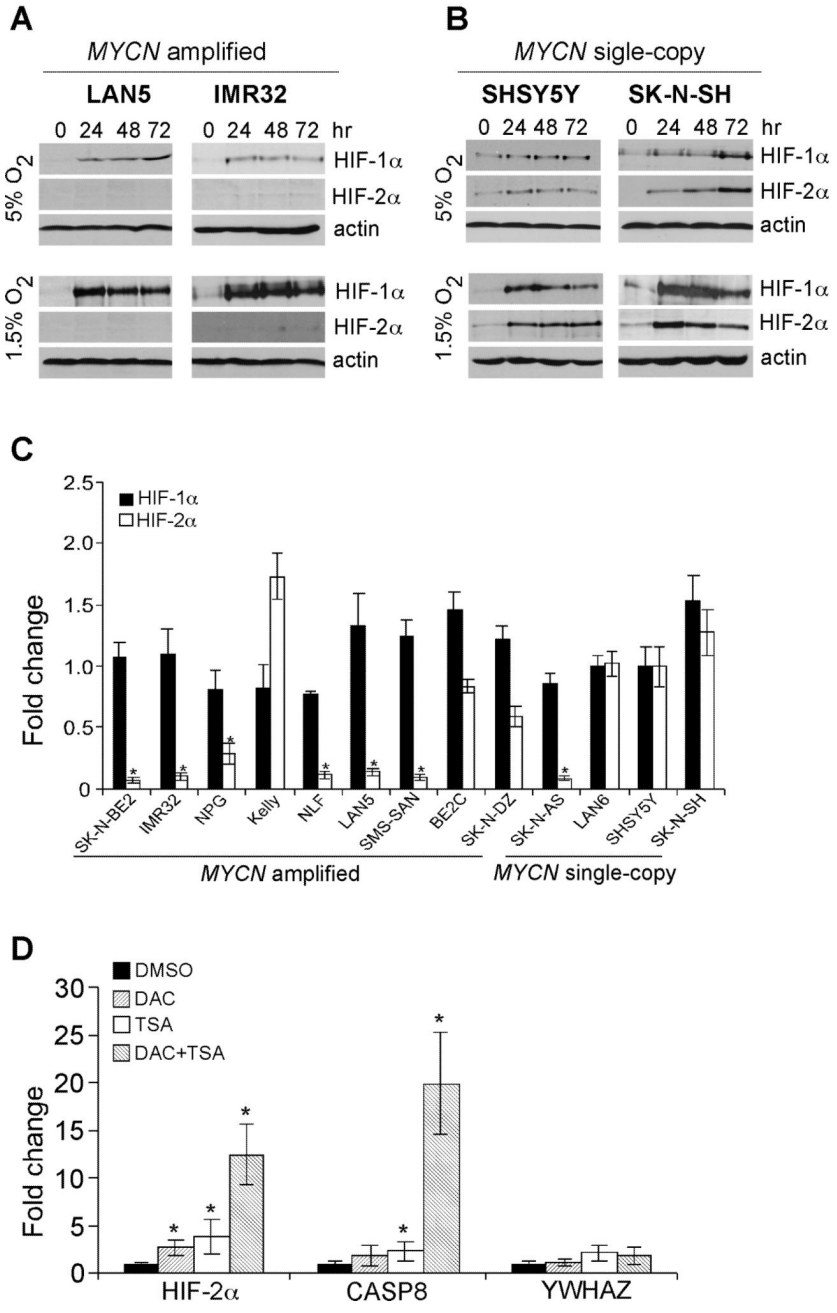

Figure 1. *MYCN* amplified neuroblastoma cells preferentially express HIF-1α

(A) Western blot analysis of HIF-α expression in LAN5 and IMR32 cells cultured at different time points under 5% O_2 and 1.5% O_2 conditions. β-actin was used as a loading control.

(B) Western blot analysis of HIF-α expression in SHSY5Y and SK-N-SH cells cultured at different time points under 5% O_2 and 1.5% O_2 conditions. β-actin was used as a loading control.

(C) Expression of HIF-α in different neuroblastoma cell lines at normoxia. The mRNA level of HIF-1α or HIF-2α in SHSY5Y cells was arbitrarily set as 1, and the relative expression of

the remaining cell lines were calculated as shown. Data are presented as an average of triplicates and normalized to β-actin mRNA. *p< 0.001.

(D) Synergistic regulation of *HIF-2A* expression by DNA methylation and histone deacetylation in *MYCN* amplified cells. LAN5 cells were either treated with vehicle or 3 μM DAC, 500 nM TSA, as well as DAC and TSA combinations. *CASP8* and *YWHAZ* were used as positive and negative controls, respectively. Data are presented as an average of triplicates. *p< 0.01.

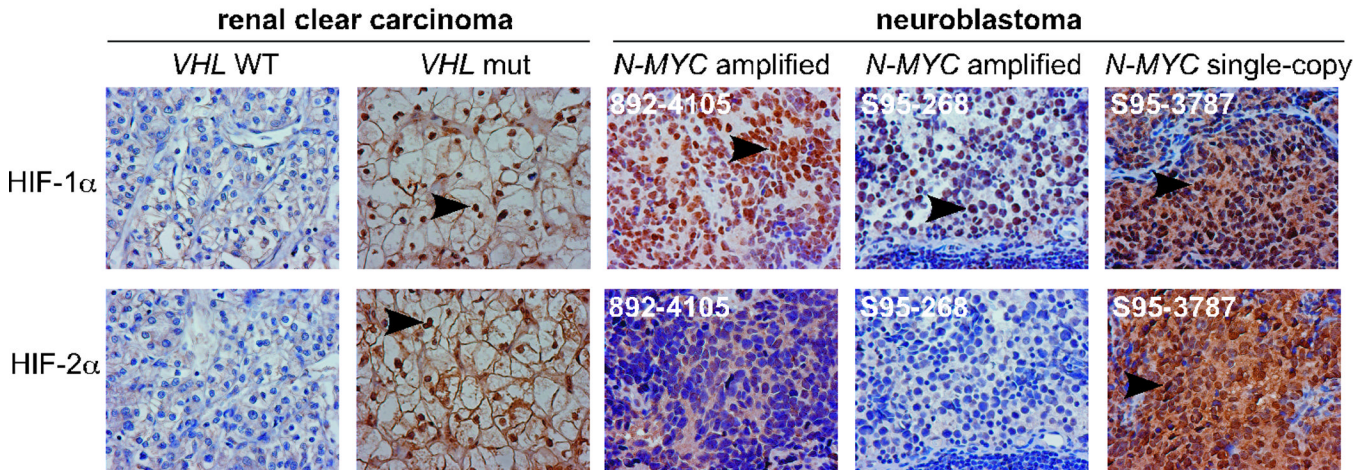

Figure 2. *MYCN* amplified neuroblastoma tumors preferentially express HIF-1α

Representative HIF-α immunochemical staining of neuroblastoma tumors. Renal clear cell carcinomas were used as controls for specific HIF-α staining. Magnification: 400×. Arrows indicate positive HIF-α staining in nuclei.

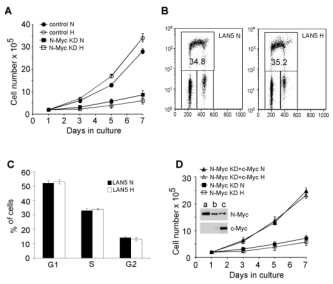

Figure 3. Proliferation of *MYCN* amplified neuroblastoma cells is maintained under hypoxia

(A) Growth of control and N-Myc knockdown LAN5 cells over seven days as measured by serial cell counts at 21% O_2 (N) and 1.5% O_2 (H).

(B) Representative FACS plots from LAN5 cells grown at 21% O_2 (N) and 1.5% O_2 (H) for 48 hr.

(C) Summary of changes in BrdU incorporation in LAN5 cells after 48 hr hypoxia. Results are averaged from 3 independent experiments.

(D) Overexpression of c-Myc rescued proliferation of N-Myc knockdown LAN5 cells. Inset: a) LAN5 cells; b) N-Myc knockdown LAN5 cells; c) N-Myc knockdown LAN5 cells with c-Myc overexpression.

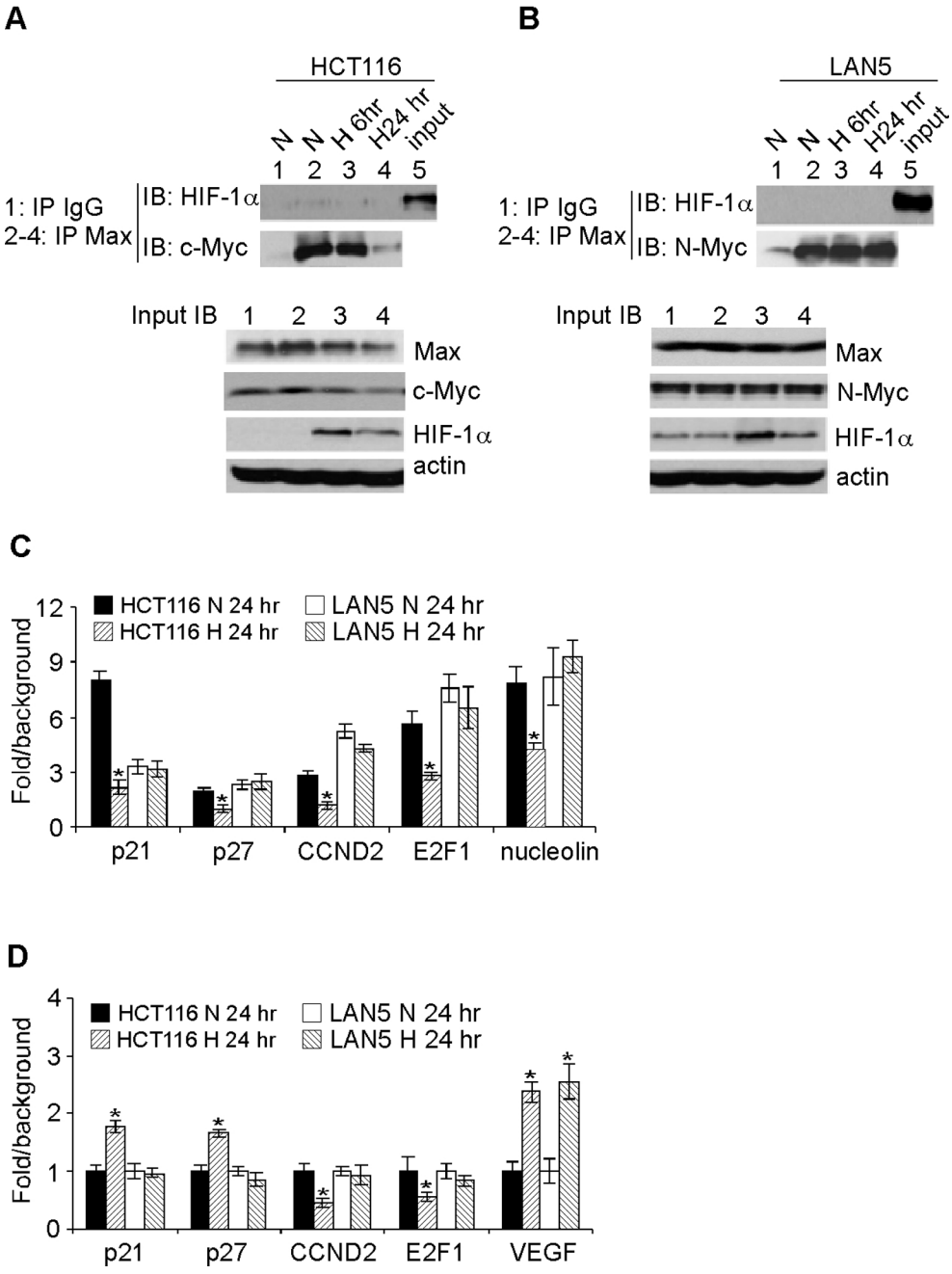

Figure 4. Changes in Myc/Max interaction and subsequent effect on target gene expression in LAN5 and HCT116 cells grown at 21% O_2 (N) and 1.5% O_2 (H)

HCT116 (A) and LAN5 (B) cell lysates from different time points were coprecipitated with Max antibody, and immunoblotted against specific c-Myc, N-Myc and HIF-1α antibodies. (C) Binding of Myc (c-Myc or N-Myc) to target promoters analyzed by ChIP assay. HCT116 and LAN5 cells were grown at 21% O_2 (N) and 1.5% O_2 (H) for 24 hr and then assayed by ChIP with specific Myc antibodies or isotype control IgG. The graphs show the fold difference between Myc IP and IgG control (background) with results obtained from triplicate assays. *p< 0.01.

(D) Expression of Myc targets involved in cell cycle progression. HCT116 and LAN5 cells were grown at 21% O_2 (N) and 1.5% O_2 (H) for 24 hr, and relative gene expression was analyzed by QRT-PCR. Results were averaged from triplicates. *$p < 0.01$.

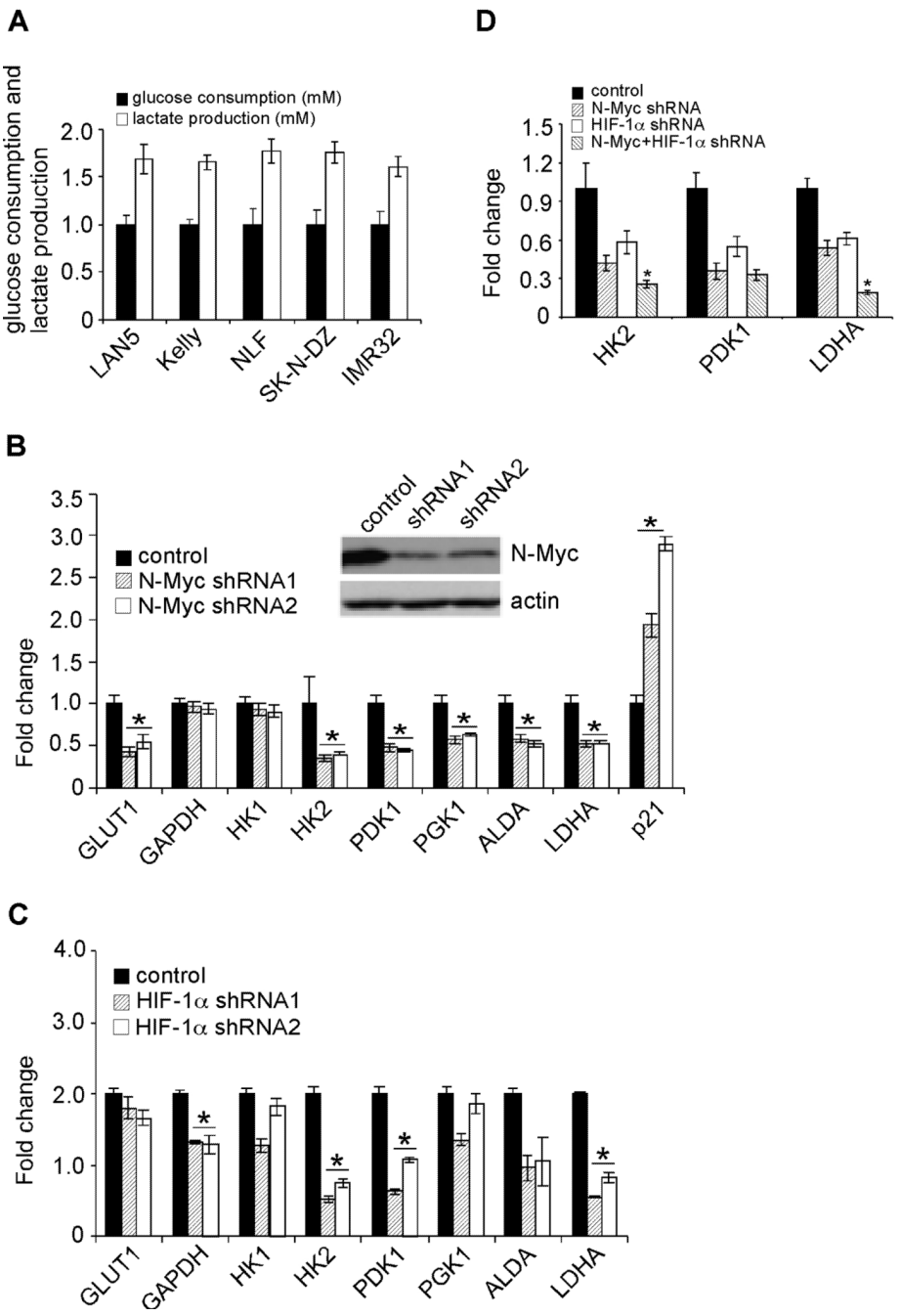

Figure 5. N-Myc and HIF-1α contribute to the Warburg effect of *MYCN* amplified neuroblastoma cells

(A) *MYCN* amplified neuroblastoma cells exhibit the Warburg phenotype. Glucose consumption and lactate production in LAN5, Kelly, NLF, SK-N-DZ and IMR32 cells cultured at normoxia for 24 hr. Data were averaged from triplicates.

(B) N-Myc regulates expression of specific genes involved in glycolysis. N-Myc was inhibited by control or specific shRNAs in LAN5 cells. Expression of glycolytic genes was determined by QRT-PCR and shown as an average of triplicates. *p< 0.001.

(C) HIF-1α regulates the expression of specific glycolytic genes at normoxia. Expression of glycolytic genes in control and HIF-1α knockdown cells was determined by QRT-PCR and shown as an average of triplicates. *p< 0.005.

(D) Effects of simultaneous HIF-1α and N-Myc inhibition on *HK2*, *PDK1* and *LDHA* expression. N-Myc and HIF-1α were depleted by control or specific shRNAs in LAN5 cells. Expression of *HK2*, *PDK1* and *LDHA* was determined by QRT-PCR and shown as an average of triplicates. *p< 0.01.

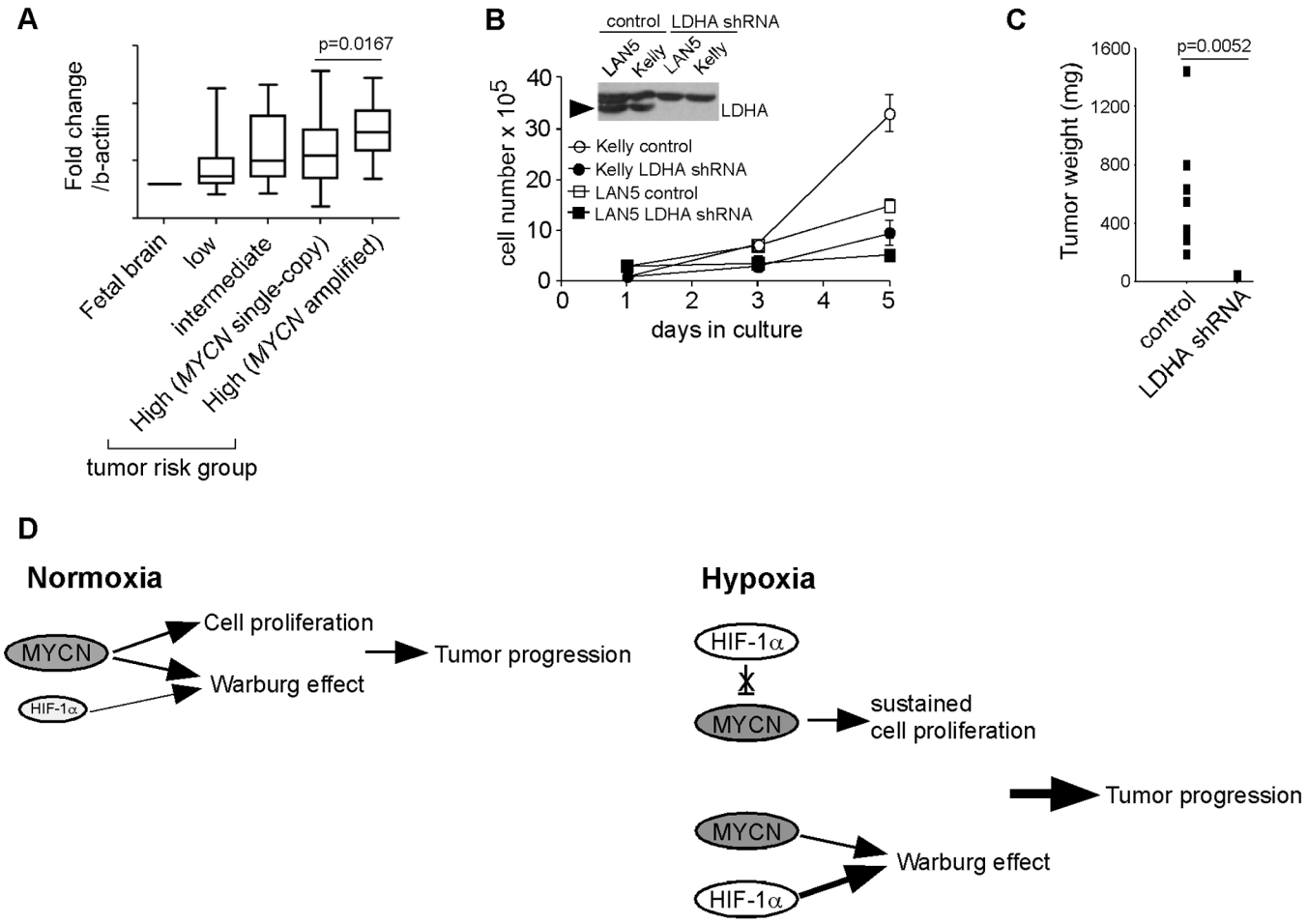

Figure 6. LDHA is a promising therapeutic target for neuroblastoma patients

(A) Relative expression of LDHA in primary neuroblastoma tumors. LDHA levels in fetal brain were used as a control. Tumor numbers: low risk group (28), intermediate (21), *MYCN* single-copy, high risk (32) and *MYCN* amplified, high risk (20).

(B) Depletion of LDHA expression profoundly inhibits the proliferation of *MYCN* amplified neuroblastoma cells. The LDHA protein is indicated by arrowhead. *p< 0.01.

(C) Depletion of LDHA expression inhibits the tumorigenic capacity of Kelly cells (8 tumors were analyzed in each group).

(D) A model depicting N-Myc and HIF-1α cooperation in neuroblastoma tumor progression. See text for details.